Kinetics of 1,3-Dipolar Cycloadditions of Dimethylacetylenedicarboxylate to Cobaloxime–Azide, $LCo(DH)_2N_3$, Complexes

BING TAI HSIEH, NICHOLAS E. TAKACH, EMIL B. MILOSAVLJEVIĆ, JOHN H. NELSON*
Department of Chemistry, University of Nevada, Reno, Nev. 89557, U.S.A.
TIMM KEMMERICH, WOLFGANG BECK*
Institut für Anorganische Chemie der Universität München, D-8000 Munich 2, F.R.G.
NEVERENKA BRESCIANI-PAHOR, LUCIO RANDACCIO*
Istituto di Chimica, Università di Trieste, 34127 Trieste, Italy
and KAY R. BROWER*
Department of Chemistry, New Mexico Institute of Mining and Technology, Socorro, N.M. 87801, U.S.A.

(Received February 4, 1987)

Abstract

The kinetics of the following 1,3-dipolar cycloaddition reactions have been studied by infrared spectroscopy

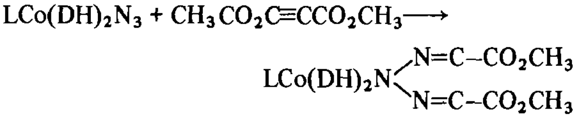

$$LCo(DH)_2N_3 + CH_3CO_2C{\equiv}CCO_2CH_3 \longrightarrow LCo(DH)_2N\begin{cases} N{=}C{-}CO_2CH_3 \\ N{=}C{-}CO_2CH_3 \end{cases}$$

where L is a variety of nitrogen and phosphorus ligands and one arsenic ligand. For all ligands except *para*-substituted triarylphosphines and tricylohexylphosphine the reaction rates are second order and are virtually unaffected by the nature of the ligand, L. For the *para*-substituted triarylphosphine and tricyclohexylphosphine complexes, the reactions are biphasic and autocatalytic. The slow step in the autocatalytic reactions is found to be an associative second order process that occurs at a rate comparable to the cycloadditions of the other $LCo(DH)_2N_3$ complexes. This slow step is followed by a faster zero order process that is independent of the $LCo(DH)_2N_3$ concentration. The rates of both steps in the autocatalytic reactions are linearly related to Hammett constants and increase with decreasing basicity of the triarylphosphine. The rates are also linearly related to the reduction potentials of the $(Ar_3P)Co(DH)_2N_3$ complexes and increase with increasing ease of reduction. It is shown that autocatalysis probably involves cobalt(II) species and a mechanism is proposed for the autocatalysis.

Introduction

The cycloaddition of 1,3-dipoles to dipolarophiles has been extensively studied [1] because of its widespread synthetic utility. We have recently reported [2] our results regarding the cycloadditions of various dipolarophiles to cobalt chelate azide complexes of the type $LCo(chelate)N_3$. This work forms part of an overall effort [3, 4] to find catalysts for reaction (1) and is based on the observations that the rates of the cycloadditions of azide ligands with various dipolarophiles depend on the metal center (Pd, Pt or Co) and both the steric and electronic properties of the other ancillary ligands [5]. We are interested in catalyzing reaction (1) because of the manifold uses of tetrazoles [6–8] in medicine, biology, agriculture, the manufacture of polymeric materials and as explosives and propellants. The traditional synthesis of tetrazoles involve 1,3-dipolar cycloadditions of nitriles to azides [6–8]. The syntheses [9] of 1,5-disubstituted tetrazoles (**1**) generally involve alkylations of the tetrazolate anion, which is formed by deprotonation of the parent tetrazole with strong base. These alkylations usually produce mixtures containing the desired 1,5-disubstituted tetrazole and substantial amounts of the isomeric 2,5-disub-

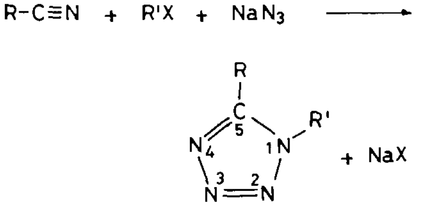

1

(1)

---

*Authors to whom correspondence should be addressed.

stituted tetrazole [9]. Separation of the more useful 1,5-disubstituted tetrazole from the 2,5-disubstituted tetrazole often requires tedius column chromatography, an industrially undesirable process. We have shown, however, that if the tetrazolate ion is coordinated to a sterically encumbered metal center, that coordination of the ambidentate tetrazolate occurs at N_2 specifically [3], and that alkylation of this N_2 coordinated tetrazolate results in the specific formation of 1,5-disubstituted tetrazoles [3, 4]. However, these same sterically encumbered transition metal centers render an azide coordinated to them so unreactive that cycloaddition to nitriles occurs only [2] with very electron deficient nitriles (e.g. CF_3CN). In contrast, cycloaddition of nitriles to coordinatively unsaturated azide complexes of palladium(II) and platinum(II) occurs under relatively mild conditions [5]. In an effort to elucidate those factors which are responsible for activation of the coordinated azide towards 1,3-dipolar cycloaddition, we have investigated the kinetics of the reactions [2] of a series [10] of $LCo(DH)_2N_3$ complexes (DH is the monoanion of dimethylglyoxime) with $CH_3CO_2C{\equiv}CCO_2CH_3$ (DAD). The results of these studies are described herein.

Experimental

Materials

Commercially available reagents were reagent grade and were used as received if they contained no NMR or IR detectable contaminants. Otherwise they were purified by standard procedures. The chloroform used for kinetic measurements was acid washed to remove the ethanol stabilizer, doubly distilled over calcium chloride, checked by ^1H NMR spectroscopy for purity, kept in the dark and used the same day it was distilled. Dimethylacetylenedicarboxylate (Aldrich) was distilled under reduced pressure (boiling point (b.p.) 90 °C, 15 mm) just prior to kinetic studies. The $LCo(DH)_2N_3$ complexes were prepared as previously described [2, 10], recrystallized three times and vacuum dried overnight at ambient temperature. Their purity was checked by infrared spectroscopy, ^1H and, where appropriate, $^{31}P\{^1H\}$ NMR spectroscopy and elemental analyses (Galbraith Laboratories, Knoxville, Tenn. 37921). All complexes gave satisfactory carbon and hydrogen analyses. Phenyl azide was synthesized by the method of Lindsay and Allen [11].

Spectroscopic Measurements

Infrared spectra were recorded on a Perkin-Elmer 599 spectrophotometer as KBr pellets and as chloroform solutions in 0.1 mm sealed NaCl cells. The ^1H and $^{31}P\{^1H\}$ NMR spectra were recorded at 99.54 and 40.26 MHz, respectively, on a JEOL-FX-100 spectrometer in the FT mode. Proton chemical shifts are downfield relative to internal Me_4Si, while the phosphorus chemical shifts were measured relative to external PPh_3 ($\delta = -6.0$ ppm) and corrected to 85% H_3PO_4. A positive sign on the phosphorus chemical shift indicates a downfield position relative to H_3PO_4.

Cyclic Voltammetry

All cyclic voltammograms were recorded at 25 ± 0.1 °C in acetonitrile containing 0.1 M tetraethylammonium perchlorate (TEAP) using an EG&G PAR electrochemistry apparatus consisting of a model RE 0073 recorder, a model 173 potentiostat and a model 175 universal programmer. A three electrode system with instrumental IR compensation was used throughout. The working electrode and auxiliary electrode were a platinum disk and wire, respectively. The reference electrode was a saturated calomel electrode, separated from the test solution by a salt bridge containing a Vycor plug and filled with 0.1 M TEAP in acetonitrile. Temperature regulation was achieved with a Brinkman Lauda K-2/R temperature controller with the electrochemical cell immersed in the constant temperature bath. As recommended by the IUPAC [12] for electrochemistry in non aqueous solvents, the ferricinium ion (Fc^+)/ferrocene (Fc) couple was employed as the reference, and all potentials reported herein are given *versus* this couple. As suggested by Gagné *et al.* [13], ferrocene was used whenever possible as an internal standard to compensate for the junction potential variability among experiments. TEAP (fluka, purum) was recrystallized from ethanol/water and dried under vacuum at 100 °C overnight. Acetonitrile (Aldrich, gold label, spectrophotometric grade) was dried over Linde 4 Å molecular sieves.

Kinetic Studies

Solutions containing 3.75×10^{-4} mol of the azide complex and 3.75×10^{-3} mol of dimethylacetylenedicarboxylate in 30 ml freshly distilled chloroform were contained in a 50 ml two-necked round bottom flask. The center neck of the flask was surmounted with a water-cooled condenser and a calcium chloride drying tube and the side neck was closed with a rubber syringe septum. The flask was immersed in a Brinkman Lauda K-2/R temperature bath maintained ($T \pm 0.1$ °C) at the desired temperature. Aliquots were withdrawn periodically from this flask by syringe and the $\nu(N_3)$-(asym) absorbance at about 2010 cm^{-1} measured as a function of time in 0.1 mm sealed NaCl cells. Three repetitive scans were made between 2100 and 2001 cm^{-1} with a 5X chart expansion and an ordinate expansion of 3. The lower energy limit was set at 2001 cm^{-1} in order to avoid a lengthy grating change at 2000 cm^{-1}. All kinetic data are the average of at least three such experiments. Beer's Law behavior was verified for the $\nu(N_3)$(asym) vibration for each complex over the concentration range studied. The reactions were followed for at least three half lives and in most cases until the reaction was 95% complete. The kinetic data were plotted and analyzed by a linear least-squares regression curve fitting computer program [14]. Plots of $\ln k/T$ *versus* T^{-1} were treated by least-squares analyses [14] to obtain $\Delta H^\ddagger$ and $\Delta S^\ddagger$ which have uncertainties of about ±0.5 kcal/mol and ±1.0 e.u., respectively.

Activation Volume Measurements

Activation volumes were obtained by studying the effects of pressure (1–1360 bar) on the reaction rates using either 1,2-dichloroethane or chloroform as solvent at 45.1 °C. The high pressure pump, gage, valves, tubing, fittings and microseries reactor were obtained from the American Instrument Co., Silver Springs, Md. The temperature of the reactor was controlled by a 100 kg aluminum ingot which was bored to fit the reactor body snugly. A thin oil film was used to improve thermal contact. The temperature of the ingot was controlled within 0.1 °C. Samples were contained in an inverted miniature glass bell which was sealed with mercury in contact with the pressure transmitting fluid (glycol). After reaction for a measured time, usually several hours, the sample was removed and placed directly in the IR liquid cell for analysis within two minutes. Activation volumes were calculated from the slope of a plot of ln k *versus* P according to the equation

$$\left(\frac{\delta \ln k}{\delta P}\right)_T = \frac{-\Delta V^\ddagger}{RT}$$

and have uncertainties of about to ±1 ml.

Results and Discussion

1. General Observations

A series of cobaloxime azide complexes, $LCo(DH)_2N_3$ (2), has previously been shown [2] to react cleanly with dimethylacetylenedicarboxylate to produce cobaloxime triazolate complexes (4), as shown in reaction (2). The rates of these reactions depend upon the nature of the ligand L.

TABLE I. Dependence of the Rate of Reaction (2) on the Concentrations of the Reactants[a]

L^b	$10^3[LCo(DH)_2N_3]$	10^2[DAD]	10^5k_{obs} (s^{-1})
DBP	6.25	12.5	1.84 ± 0.05
DBP	12.5	12.5	1.47 ± 0.05
DBP	12.5	25.0	3.01 ± 0.05
pip	6.25	12.5	0.83 ± 0.05
pip	12.5	12.5	1.01 ± 0.05
pip	12.5	25.0	1.92 ± 0.05
Ph_3As	6.25	12.5	0.59 ± 0.05
Ph_3As	12.5	12.5	0.68 ± 0.05
Ph_3As	12.5	25.0	1.30 ± 0.05

[a] In $CHCl_3$ at 27 °C. [b] DBP = 1-phenyldibenzophosphole, pip = piperidine.

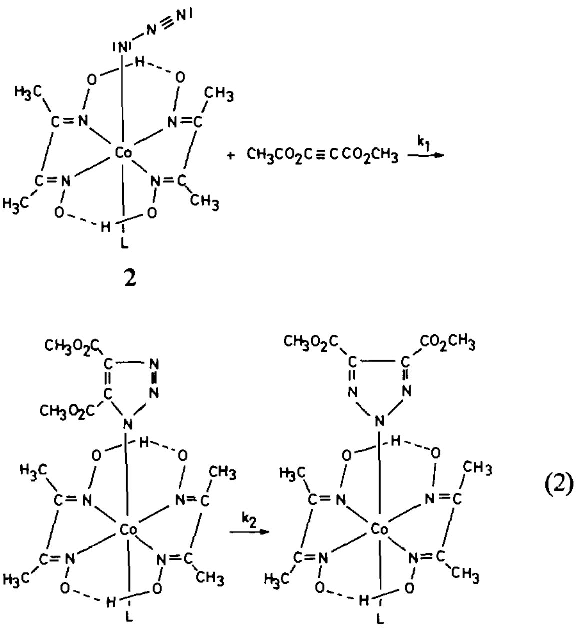

Although 3 is probably the first-formed product of these 1,3-dipolar cycloadditions, no spectroscopic evidence for this species could be obtained. In each case, the isolated product is 4. The crystal structures of $PPh_3Co(DH)_2N_3$ and

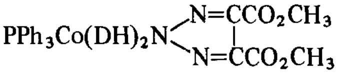

$$PPh_3Co(DH)_2N\begin{cases}N{=}CCO_2CH_3\\ \quad\ |\\ N{=}CCO_2CH_3\end{cases}$$

have previously been reported elsewhere [15]. These confirm the general structural drawings 2 and 4 with $L = PPh_3$.

The rates of reaction (2) have been investigated under pseudo first order conditions. Infrared spectroscopic monitoring was used to follow the decrease in intensity of the $\nu(N_3)$(asym) vibration for the $LCo(DH)_2N_3$ complexes in the presence of a ten to one molar ratio of DAD to complex. The data of Table I show that the reactions are first order in DAD; thus the reactions are overall second order, first order in each reactant. Similar behavior was found for all the complexes listed in Table II. The data conform to the rate law: rate = $k_{obs}[LCo(DH)_2N_3]$ where $k_{obs} = k'$[DAD]. Figure 1 shows a typical pseudo first order plot of $\ln[LCo(DH)_2N_3]$ (measured as $\ln A/A_0\nu(N_3)$(asym) *versus* time. As the data in Table II show, the rates of these reactions are not very sensitive to the nature of the ligand *trans* to the azide. The fastest reaction ($L = Me_2PPh$) is only 3.5 times as fast as the slowest ($L = (C_6H_5)_3$-

TABLE II. Rate Data for the Reactions: $LCo(DH)_2N_3 + CH_3CO_2C{\equiv}CCO_2CH_3 \rightarrow LCo(DH)_2$triazolate in Chloroform at 27 °C[a]

L	$10^5 k_{obs}$ (s^{-1})
Me_2PPh	2.38 ± 0.05
$(C_2H_5O)_3P$	1.77 ± 0.05
1-methylimidazole	1.56 ± 0.05
DBP	1.47 ± 0.05
$MePPh_2$	1.32 ± 0.05
$P(n\text{-}Bu)_3$	1.30 ± 0.05
$(PhCH_2)_3P$	1.21 ± 0.05
$(C_6H_5O)_3P$	1.11 ± 0.05
Piperidine	1.01 ± 0.05
Pyridine	0.734 ± 0.005
$(C_6H_5)_3As$	0.680 ± 0.005

[a] $[LCo(DH)_2N_3]$ = 0.0125 M; $[CH_3CO_2C{\equiv}CCO_2CH_3]$ = 0.125 M; $k' = k_{obs}/[DAD] \approx 0.69/t_{1/2}$.

As) and the half lives only span the range of 8.1 to 28.3 h at 27 °C.

The activation parameters for the reactions of $PyCo(DH)_2N_3$ ($\Delta H^{\ddagger}$ = 11.9 kcal/mol, $\Delta S^{\ddagger}$ = −38 e.u.) and $[(PhCH_2)_3P]Co(DH)_2N_3$ ($\Delta H^{\ddagger}$ = 13.4 kcal/mol, $\Delta S^{\ddagger}$ = −33 e.u.) are consistent with what would be expected for an associative process and are similar to those previously found [16] for the reaction of phenyl azide with DAD ($\Delta H^{\ddagger}$ = 17.4 kcal/mol, $\Delta S^{\ddagger}$ = −26 e.u.). Similar activation parameters have also been reported for cycloaddition reactions of azidoplatinum(II) complexes with nitriles [5b].

In contrast to the reactions discussed above, the reactions of the complexes $LCo(DH)_2N_3$, where L is a triarylphosphine, are biphasic and autocatalytic, increasing in rate with time as illustrated in Fig. 2. As the data in Table III show, the initial stage in these reactions is second order overall, first order in each reactant, with an associated second order rate constant $k' = k_s/[DAD]$ that is comparable to the rate constants found for the other $LCo(DH)_2N_3$ reactions discussed above. Compare k_{obs}

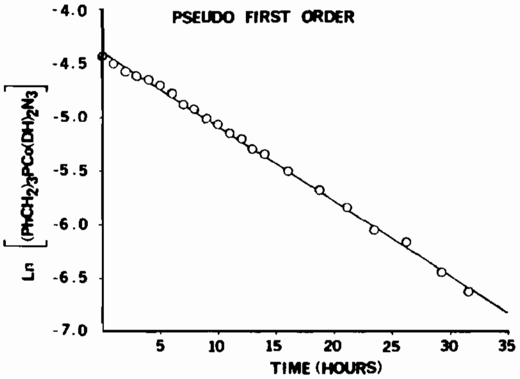

Fig. 1. Pseudo first order rate plot for the reaction of $(PhCH_2)_3PCo(DH)_2N_3$ (0.0125 M) with $CH_3CO_2C{\equiv}CCO_2CH_3$ (0.125 M) in $CHCl_3$ at 27 °C. Similar data were obtained for all the complexes listed in Table II.

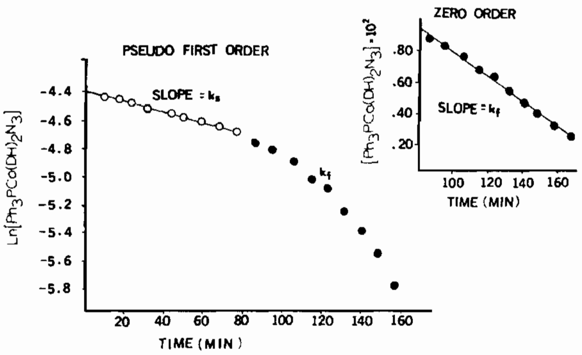

Fig. 2. Biphasic kinetic plot for the reaction of $PPh_3Co(DH)_2N_3$ with $CH_3CO_2C{\equiv}CCO_2CH_3$ in $CHCl_3$ at 22 °C. Open circles represent the pseudo first order slow step (k_s) and solid circles represent the zero order fast step (k_f). Similar data were obtained for all the complexes listed in Table IV.

TABLE III. Dependence of the Rate of Reaction (2) on the Concentrations of the Reactants where L is a Triarylphosphine $(p\text{-}XC_6H_4)_3P$ or Tricyclohexylphosphine, Cy_3P, in $CHCl_3$ at 27 °C

X	$10^3[LCo(DH)_2N_3]$	$10^2[DAD]$	$10^5 k_s$ (s^{-1})	$10^6 k_f$ ($M\ s^{-1}$)
H	6.25	12.5	6.95 ± 0.05	1.89 ± 0.05
H	12.5	12.5	6.94 ± 0.05	2.23 ± 0.05
H	25.0	25.0	14.1 ± 0.5	4.16 ± 0.05
CH_3	6.25	12.5	2.29 ± 0.05	0.352 ± 0.005
CH_3	12.5	12.5	1.88 ± 0.05	0.948 ± 0.005
CH_3	25.0	25.0	4.40 ± 0.05	2.47 ± 0.05
CH_3O	6.25	12.5	1.03 ± 0.05	0.211 ± 0.005
CH_3O	12.5	12.5	1.18 ± 0.05	0.231 ± 0.005
CH_3O	25.0	25.0	2.22 ± 0.05	0.48 ± 0.05
			$10^4 k_{obs}$ (s^{-1})	
Cy_3P	6.25	12.5	2.83 ± 0.05	
Cy_3P	12.5	12.5	2.86 ± 0.05	
Cy_3P	25.0	25.0	4.87 ± 0.05	

TABLE IV. Rate Data for the Reactions: $(p\text{-}XC_6H_4)_3PCo(DH)_2N_3 + CH_3CO_2C{\equiv}CCO_2CH_3 \rightarrow (p\text{-}XC_6H_4)_3PCo(DH)_2$triazolate in Chloroform at 27 °C[a]

X	$\Sigma\sigma p$[b]	$10^5 k_s$ (s^{-1})[c]	$10^7 k_f$ ($M\ s^{-1}$)[d]	Completion time (min)[e]
Cl	0.69	56.7 ± 0.5	66.8 ± 0.5	31
H	0	6.94 ± 0.05	22.30 ± 0.5	120
CH_3	−0.51	1.88 ± 0.05	9.48 ± 0.05	334
CH_3O	−0.81	1.18 ± 0.05	2.31 ± 0.05	966

[a] $[LCo(DH)_2N_3]$ = 0.0125 M; $[CH_3CO_2C{\equiv}CCO_2CH_3]$ = 0.125 M. [b] Ref. 36. [c] $\log(kX/kH) = \rho\Sigma\sigma p$; $\rho = +1.14$; pseudo first order rate constants ($r^2 = 0.99$). [d] $\log(kX/kH) = \rho\Sigma\sigma p$; $\rho = +0.91$; zero order rate constants ($r^2 = 0.94$). [e] Calculated by extrapolating the experimental rate plots to zero concentration.

in Table II with k_s given in Table III. Also, the activation parameters found for the initial stage in the reaction of $(PPh_3)Co(DH)_2N_3$ ($\Delta H^{\ddagger} = 9.9$ kcal/mol, $\Delta S^{\ddagger} = -41$ e.u.) are similar to those found for the reactions of the $pyCo(DH)_2N_3$ and $[(PhCH_2)_3P]Co(DH)_2N_3$ complexes. The initial stage is followed by a faster zero order process wich is independent of $[LCo(DH)_2N_3]$.

2. *Autocatalysis*

Several experiments have been conducted to gain some understanding of the nature of the autocatalysis responsible for the fast step in these reactions. The rates of both the slow initial stage and the faster second stage are both linearly related to Hammett substituent parameters (Table IV). In both cases the rate increases with a decrease in the basicity of the phosphine and ρ is slightly greater for the initial stage. Since these reactions are autocatalytic, the $Ar_3PCo(DH)_2$triazolate product could be the source of the catalyst. The crystallographic data [15] for $PPh_3Co(DH)_2N_3$ and $PPh_3Co(DH)_2$triazolate show that the triazolate has a greater *trans* influence [17–19] than does azide. The cobalt–phosphorus bond is longer (2.333(1) *versus* 2.311(1) Å) and the cobalt–nitrogen bond is shorter (1.953(3) *versus* 2.014(4) Å) in the triazolate complex than in the azide complex. We have previously shown [2] that PPh_3 readily dissociates from the triazolate complex and isolation of $PPh_3Co(DH)_2$triazolate requires addition of excess PPh_3. It is known [20–22] that triphenylphosphine and some other phosphines react rapidly and irreversibly with DAD according to reaction (3) to form transient carbenoid species which ultimately yield dimeric and polymeric products. This carbenoid species could reduce the $LCo^{III}(DH)_2N_3$ complex to the cobalt(II) analog by an inner sphere electron transfer [23]*. It is not possible to prepare the cobalt(II) triazolate complex. Thus, in order to establish that the catalyst was derived from the $R_3PCo(DH)_2$triazolate, it was added to the reaction solution and the kinetics followed in its presence. A solution containing 0.0125 M $PPh_3Co(DH)_2N_3$; 0.125 M DAD and 0.0125 M $PPh_3Co(DH)_2$triazolate had zero order kinetic behavior (Fig. 3). The zero order rate constant was 4.03 X 10^{-6} m s^{-1} (*cf.* Table V); the time to completion was 52 min compared to a completion time of 120 min in the absence of the triazolate complex. Thus the triazolate complex catalyzes the reaction. In order to show that the reaction is catalyzed by cobalt(II), as has been observed [24] for ligand exchange reactions of cobalt(III) oxime complexes, we added the cobalt(II) complex $(PPh_3)_2Co(DH)_2$ [25] to the reaction. A solution containing 0.0125 M $PPh_3Co(DH)_2N_3$; 0.125 M DAD and 0.0125 M. $(PPh_3)_2Co(DH)_2$ showed zero order rate behavior with zero order rate constant of 4.32 X 10^{-6} m s^{-1}.

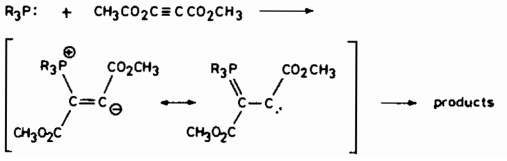

(3)

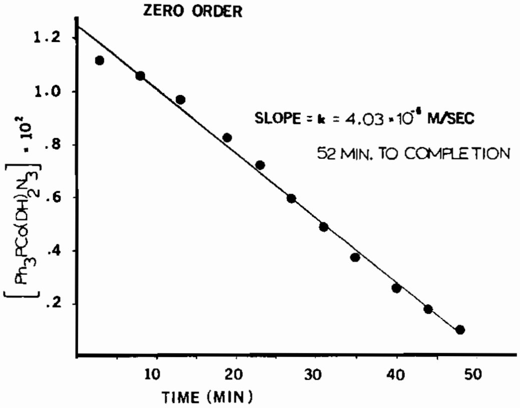

Fig. 3. Kinetic plot for the reaction of $PPh_3Co(DH)_2N_3$ with $CH_3CO_2C{\equiv}CCO_2CH_3$ in the presence of $PPh_3Co(DH)_2$triazolate in $CHCl_3$ at 27 °C. Zero order plot.

---

*Usually, the bridging ligand transfers from oxidant to reductant during an inner sphere redox reaction. However, there is no bridging ligand transfer in the inner sphere electron exchange mechanism proposed here.

TABLE V. Rate Data for the Reactions: $(PPh_3)Co(DH)_2N_3 + CH_3CO_2C{\equiv}CCO_2CH_3 \rightarrow PPh_3Co(DH)_2$triazolate in Chloroform at 27 °C[a]

Solvent	Catalyst	$10^5 k_s$ (s^{-1})	$10^6 k_f$ (M s^{-1})	Completion time (min)[e]
$CHCl_3$	none	6.94[c] ± 0.05	2.23 ± 0.05	120
$CHCl_3$	0.0125 M $PPh_3Co(DH)_2$TRI		4.03 ± 0.05	52
$CHCl_3$	0.0125 M $(PPh_3)_2Co(DH)_2$		4.32 ± 0.05	48
$CHCl_3$[b]	0.0125 M $(PPh_3)_2Co(DH)_2$		3.26 ± 0.05	32
95% $CHCl_3$ and 5% $CBrCl_3$	none	1.41[d] ± 0.05		

[a] $[PPh_3Co(DH)_2N_3]$ = 0.0125 M; $[CH_3CO_2C{\equiv}CCO_2CH_3]$ = 0.125 M. [b] $[PPh_3Co(DH)_2N_3]$ = 0.00625 M; $[CH_3CO_2C{\equiv}CCO_2CH_3]$ = 0.125 M. [c] $t_{1/2}$ = 2.8 h; but because k_f is also contributing $t_{1/2}$ = 1 h. [d] $t_{1/2}$ = 13.7 h. [e] Calculated by extrapolating the experimental rate plots to zero concentration.

Under otherwise identical conditions the zero order rate constant was lowered to 3.26×10^{-6} M s^{-1} when the $(PPh_3)_2Co(DH)_2$ concentration was reduced to 6.25×10^{-3} M. These rate constants are not directly proportional to the $(PPh_3)_2Co(DH)_2$ concentration because PPh_3 must first dissociate from the cobalt(II) complex before the latter may enter into sphere electron transfer with $PPh_3Co(DH)_2N_3$; the fraction of $(PPh_3)Co(DH)_2$ present depends upon the initial concentration of $(PPh_3)_2Co(DH)_2$. Furthermore, the liberated PPh_3 can react with DAD according to reaction (3) and can also serve to decrease the extent of dissociation of PPh_3 from the reaction product $PPh_3Co(DH)_2$triazolate. An additional test for cobalt(II) catalysis may be obtained from a rate retardation by the mild oxidizing agent $CBrCl_3$ [24]. Thus, we find (Table V) that in the presence of 5% $CBrCl_3$ pseudo first order behavior is exhibited throughout the reaction with a pseudo first order rate constant of 1.41×10^{-5} s^{-1}. Each of the kinetic infrared spectra of the autocatalytic reactions exhibit a new minor N_3 stretching vibration which reaches a maximum intensity near the midpoint of the reactions and decreases to zero afterwards. This vibration is clearly due to some intermediate species. The frequency of this new vibration is approximately 25 cm^{-1} higher than the $\nu(N_3)$(asym) of the starting $LCo(DH)_2N_3$ complex. This vibration could be due to either a cobalt(II) azide or a $Co(II)N_3Co(III)$ bridged dimer. The above results suggest that the autocatalysis involves a cobalt(II) species that is derived from the $PPh_3Co(DH)_2$triazolate product.

Other cobalt chelate complexes of the type $PPh_3Co(chelate)N_3$, show an increasing tendency to dissociate the ligand PPh_3 to form the ligand free complexes as the donor strength of the chelate system increases [26, 27]. Parallel to this, one finds greatly increased cycloaddition rates [28] for these complexes. Though $P(OPh)_3$ and $AsPh_3$ also dissociate from the $LCo(DH)_2$triazolate complexes [2], the reactions of these two complexes are not autocatalytic. This may be explained by the fact that $P(OPh)_3$ and $AsPh_3$ are not good enough nucleophiles to react with DAD and generate carbenoid species by reaction (3).

We were unable to verify phosphine dissociation from any of the triazolate complexes by ^{31}P NMR spectroscopy. The ^{31}P NMR spectra showed only a very small change in chemical shifts for these complexes in the presence of excess phosphine. This is probably because the line widths are very broad (*ca.* 100 Hz) due to cobalt quadrupole broadening [3], together with ligand exchange effects.

For the autocatalytic reactions, the autocatalysis commences as soon as some product is formed. Thus, there is some contribution of both the slow initial and faster follow up stages throughout the reaction. As a result, we probably overestimated k_s and underestimated k_f. We believe that these errors are small; we have not attempted a more rigorous data analysis. The above results suggest that excess phosphine should affect the rates of these reactions.

Thus, the reaction of the $PPh_3Co(DH)_2N_3$ complex was studied in the presence of varying concentrations of excess PPh_3. It was found (Table VI) that addition of phosphine increased the rate of the slow pseudo first order process. At present, we have no good explanation for this observation. Perhaps there is an increased contribution of the fast step in the early part of the reaction in the presence of excess PPh_3. The rate of the following fast step was also increased by excess PPh_3. The fast step seems to involve dissociation of PPh_3 from the product, $PPh_3Co(DH)_2$triazolate, and subsequent formation of $[PPh_3Co(DH)_2N_3]^-$ by inner sphere electron transfer. For it, added PPh_3 first increased the rate up to a ratio of 1:2 PPh_3:complex, but then with increasing PPh_3 concentration the reaction rate decreased. This is probably due to two compensating effects. Additional PPh_3 increases the amount of the carbenoid species (reducing agent) by reaction (3) but also reduces the extent of PPh_3 dissociation from the product $PPh_3Co(DH)_2$triazolate. The effect is small, which is consistent with a large value for the equilibrium constant for PPh_3 dissociation.

TABLE VI. Influence of Added PPh_3 on the Rate of the Reaction: $PPh_3Co(DH)_2N_3 + CH_3CO_2C{\equiv}CCO_2CH_3 \rightarrow PPh_3Co(DH)_2$-triazolate in Chloroform at 31 °C[a]

10^3 [PPh_3]	$\frac{[PPh_3]}{[PPh_3Co(DH)_2N_3]}$	$10^5 k_s$ (s^{-1})[b]	$10^6 k_f$ ($M\ s^{-1}$)[c]
0	0	5.01 ± 0.05	2.84 ± 0.05
6.25	0.5	7.39 ± 0.05	4.30 ± 0.05
12.5	1	17.1 ± 0.5	5.00 ± 0.05
25.0	2	38.0 ± 0.5	4.70 ± 0.05
50.0	4	27.6 ± 0.5	3.60 ± 0.05

[a] [$PPh_3Co(DH)_2N_3$] = 0.00833 M; [$CH_3CO_2C{\equiv}CCO_2CH_3$] = 0.0833 M. [b] Pseudo first order rate constant. [c] Zero order rate constant.

TABLE VII. Rate Data for the Reactions: $(PhCH_2)_3PCo(DH)_2N_3 + CH_3CO_2C{\equiv}CCO_2CH_3 \rightarrow (PhCH_2)_3PCo(DH)_2$triazolate in Chloroform at 31 °C[a]

Solvent	Catalyst	$10^5 k_s$ (s^{-1})[b]	$10^6 k_f$ ($M\ s^{-1}$)[c]	$t_{1/2}$ (h)	Completion time (min)
$CHCl_3$	none	1.99 ± 0.05		9.7	
95%$CHCl_3$ and 5%$CBrCl_3$	none	1.59 ± 0.05		12.1	
$CHCl_3$	0.00125 M $(PhCH_2)_3P$	1.35 ± 0.05		14.3	
$CHCl_3$	0.0125 M $(PPh_3)_2Co(DH)_2$		3.73 ± 0.05		56
$CHCl_3$[d]	0.0125 M $(PPh_3)_2Co(DH)_2$		3.83 ± 0.05		28

[a] [$(PhCH_2)_3PCo(DH)_2N_3$] = 0.0125 M; [$CH_3CO_2C{\equiv}CCO_2CH_3$] = 0.125 M. [b] Pseudo first order rate constant. [c] Zero order rate constant. [d] [$(PhCH_2)_3PCo(DH)_2N_3$] = 0.00625 M.

The reaction of $Cy_3PCo(DH)_2N_3$ displayed slightly different behavior. At 27 °C the reaction was pseudo first order and monophasic from beginning to end. In the presence of added oxidizing agent, 5% $CBrCl_3$ in $CHCl_3$, the reaction was slowed considerably and was still pseudo first order. The pseudo first order rate constants at 27 °C when [$Cy_3PCo(DH)_2N_3$] = 0.0125 M, [DAD] = 0.125 M are $k = 2.86 \times 10^{-4}$ s^{-1} and 7.20×10^{-6} s^{-1} respectively. At 22 °C the reaction was perceptibly biphasic with $k_s = 1.07 \times 10^{-4}$ s^{-1} and $k_f = 2.00^{-4}$ s^{-1}; both steps are pseudo first order. The activation parameters for the slow step ($\Delta H^{\ddagger} = 17.7$ kcal/mol, $\Delta S^{\ddagger} = -12$ e.u.) are similar to those for the reactions listed in Table II suggesting that this reaction is also an associative second order reaction consistent with the data given in Table III.

The observation that the $Ar_3PCo(DH)_2N_3$ reactions are catalyzed by cobalt(II) species suggested that it should be possible to catalyze the other reactions by cobalt(II) species as well. The results of such a study are given in Table VII. These data show that the mild oxidizing agent $CBrCl_3$ reduces the rate of the cycloaddition of DAD to $(PhCH_2)_3PCo(DH)_2N_3$ but by a much smaller amount than was found for the $PPh_3Co(DH)_2N_3$ reaction (Table V). In the former case, there is only a 20% decrease in the reaction rate in the presence of the oxidizing agent, whereas in the latter case the rate was reduced by a factor of about five. Clearly there is little contribution of the cobalt(II) catalyzed pathway in the former case. The rate change caused by $CBrCl_3$ is probably due solely to a solvent effect [29]. The rate is also decreased somewhat by the presence of excess $(PhCH_2)_3P$, but this is probably due to the reaction of the good nucleophile $(PhCH_2)_3P$ with DAD thereby reducing the concentration of DAD by reaction (3). Because the reaction is first order in [DAD], this reaction reduces the rate. In the presence of the cobalt(II) complex, $(PPh_3)_2Co(DH)_2$, the reaction becomes zero order as was found for the $PPh_3Co(DH)_2N_3$ complex in the presence of added $(PPh_3)_2Co(DH)_2$. The rate increases only slightly with an increase in the cobalt(II) to cobalt(III) complex ratio.

Activation volumes were determined for the reaction of a representative complex in each category. The data are given in Table VIII and Fig. 4. For phenylazide $\Delta V^{\ddagger} = -13$ ml and for $pyCo(DH)_2N_3$ $\Delta V^{\ddagger} = -16$ ml. For the reaction of PhN_3 with DAD ΔV was found to be -19 ml. Thus, it appears that the transition state is closer to the product than to the reactant. The negative sign for $\Delta V^{\ddagger}$ is consistent with an associative process. Interestingly, for $PPh_3Co(DH)_2N_3$ the fast ($\Delta V^{\ddagger} = +15$ ml) and slow ($\Delta V^{\ddagger} = -14$ ml) steps have activation volumes that are nearly equal in magnitude and opposite in sign and at high pressure the reaction seems to be second order throughout (Fig. 4). Here is a case where a change in pressure affects the mechanism of the

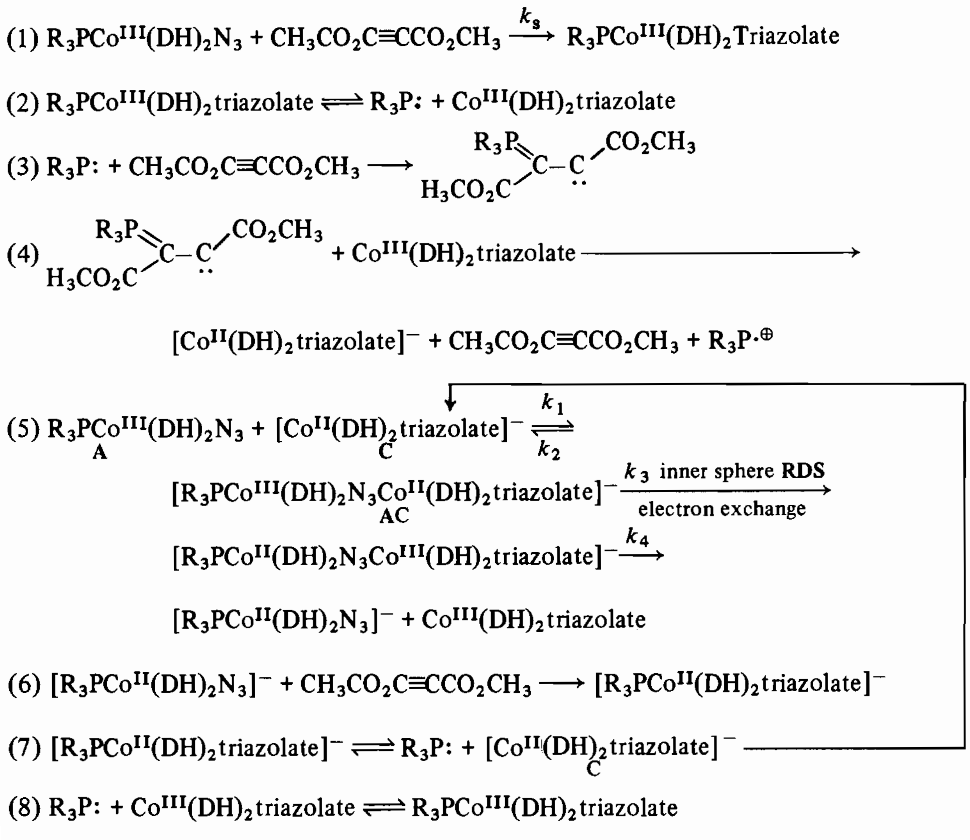

(1) $R_3PCo^{III}(DH)_2N_3 + CH_3CO_2C{\equiv}CCO_2CH_3 \xrightarrow{k_s} R_3PCo^{III}(DH)_2Triazolate$

(2) $R_3PCo^{III}(DH)_2triazolate \rightleftharpoons R_3P{:} + Co^{III}(DH)_2triazolate$

(3) $R_3P{:} + CH_3CO_2C{\equiv}CCO_2CH_3 \longrightarrow (R_3P)(H_3CO_2C)C{=}\ddot{C}{-}CO_2CH_3$

(4) $(R_3P)(H_3CO_2C)C{=}\ddot{C}{-}CO_2CH_3 + Co^{III}(DH)_2triazolate \longrightarrow [Co^{II}(DH)_2triazolate]^- + CH_3CO_2C{\equiv}CCO_2CH_3 + R_3P^{\cdot\oplus}$

(5) $\underset{A}{R_3PCo^{III}(DH)_2N_3} + \underset{C}{[Co^{II}(DH)_2triazolate]^-} \underset{k_2}{\overset{k_1}{\rightleftharpoons}} \underset{AC}{[R_3PCo^{III}(DH)_2N_3Co^{II}(DH)_2triazolate]^-} \xrightarrow[\text{electron exchange}]{k_3\ \text{inner sphere RDS}} [R_3PCo^{II}(DH)_2N_3Co^{III}(DH)_2triazolate]^- \xrightarrow{k_4} [R_3PCo^{II}(DH)_2N_3]^- + Co^{III}(DH)_2triazolate$

(6) $[R_3PCo^{II}(DH)_2N_3]^- + CH_3CO_2C{\equiv}CCO_2CH_3 \longrightarrow [R_3PCo^{II}(DH)_2triazolate]^-$

(7) $[R_3PCo^{II}(DH)_2triazolate]^- \rightleftharpoons R_3P{:} + \underset{C}{[Co^{II}(DH)_2triazolate]^-}$

(8) $R_3P{:} + Co^{III}(DH)_2triazolate \rightleftharpoons R_3PCo^{III}(DH)_2triazolate$

Scheme 1.

TABLE VIII. Effect of Pressure on Reaction Rate Constants[a]

Phenyl azide + DAD (0.28 M) in cyclohexane at 45.1 °C				
P (MPa)	7	40	73	133
10^5k (s^{-1})	2.14	2.53	2.65	3.70
$PyCo(DH)_2N_3$ + DAD (0.14 M) in chloroform at 45.1 °C				
P (MPa)	7	73	8	133
10^5k (s^{-1})	4.52	6.90	7.78	9.78

[a] Average of 1–5 measurements at each pressure, $k \pm 5 \times 10^{-7}$.

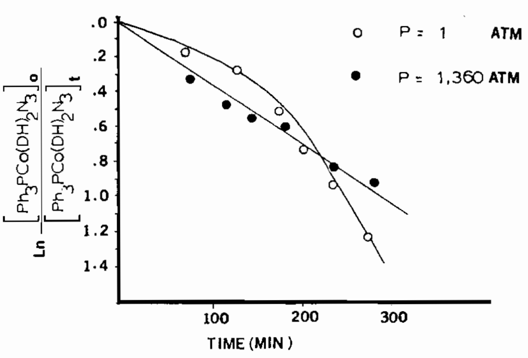

Fig. 4. Kinetic plot for the reaction of $PPh_3Co(DH)_2N_3$ with $CH_3CO_2C{\equiv}CCO_2CH_3$ in 1,2-dichloroethane at 41 °C as a function of pressure (open circles, 1 bar; closed circles, 1, 360 bar).

reaction. The increase in pressure probably decreases the extent of Ph_3P dissociation from $PPh_3Co(DH)_2$-triazolate inhibiting the autocatalysis.

3. *Autocatalysis Mechanism*

At this point it is clear that the autocatalysis mechanism involves a cobalt(II) species derived from the $Ar_3PCo(DH)_2$triazolate product. A possible mechanism for the autocatalysis is given in Scheme 1. If we assume that the rate determining step in the reaction is the inner sphere electron transfer (step 5) then

$$\text{Rate} = k_3[AC]^-$$

If we further assume a steady state concentration of $[AC^-]$ then

$$k_1([C)]_{\text{total}} - [AC]^-)[A] = (k_2 + k_3)[AC]^-$$

or

$$\frac{([C]_{\text{total}} - [AC]^-)[A]}{[AC]} = \frac{k_2 + k_3}{k_1} = k_m$$

and

$$[AC]^- = \frac{[C]_{\text{total}}[A]}{k_m + [A]}$$

or

$$\text{rate} = \frac{k_3\,[\mathrm{C}]_{\mathrm{total}}\,[\mathrm{A}]}{k_{\mathrm{m}} + [\mathrm{A}]}$$

$$= \frac{k_3[\mathrm{Co^{II}(DH)_2triazolate}]^-_{\mathrm{total}}\,[\mathrm{R_3PCo^{III}(DH)_2N_3}]}{k_{\mathrm{m}} + [\mathrm{R_3PCo^{III}(DH)_2N_3}]}$$

Now since $K_{\mathrm{m}} \ll [\mathrm{R_3PCo^{III}(DH)_2N_3}]$, the rate is independent of $[\mathrm{R_3PCo^{III}(DH)_2N_3}]$ and depends upon $[\mathrm{Co^{II}(DH)_2triazolate}]^-$ or rate $= k_3\,[\mathrm{Co^{II}(DH)_2triazolate}] = k_{\mathrm{f}}$ which is in agreement with the experimental observations.

Step (5) in Scheme 1 can be written in a simplified form as follows:

$$\mathrm{R_3PCo^{III}(DH)_2N_3} + [\mathrm{Co^{II}(DH)_2triazolate}]^- \xrightarrow{k_5} [\mathrm{R_3PCo^{II}(DH)_2N_3}]^- + \mathrm{Co^{III}(DH)_2triazolate}$$

This is because any bimolecular redox reaction of this type may be broken up into a number of steps beginning with adduct formation, k_1, (substitution) followed by electron transfer, k_3, and terminating with a substitution reaction, k_4. Writing step (5) in the simplified form we have the relation

$$k_5 = k_1 k_3/(k_2 + k_3)$$

The simplified form, however, does not show as clearly as does the more complicated form the nature of the rate determining step.

4. Electrochemistry

In order to obtain further support for the participation of cobalt(II) in the autocatalysis, cyclic voltammetry experiments have been performed on all the azide complexes and on several of the triazolate complexes. The potentials corresponding to the redox processes Co(III) ⇌ Co(IV) and Co(III) ⇌ Co(II), which were accessible with the solvent/electrolyte/electrode system used, are summarized in Table IX. The redox behavior of some similar cobalt(II)–bisdimethylglyoximato complexes has been investigated earlier [27, 30–32].

The usual diagnostic criteria utilized in cyclic voltammetry [33] point out that the mechanisms of the oxidation and reduction of the Co(III) species, when uncomplicated by the dissociation of the ligand L from the starting Co(III) complex (*vide supra*), are EC. The reversible or quasi-reversible electron transfer is followed by an irreversible chemical step*, which is probably the dissociation of the ligand L. For some of these complexes, ligand dissociation may be substantiated by the observation of the irreversible anodic wave due to the oxidation of the free ligand [L = $(p\text{-CH}_3\text{C}_6\text{H}_4)_3\text{P}$; $(\text{C}_6\text{H}_5)_3\text{As}$]. The same type of redox mechanism has been established previously for some organometallic derivatives of cobalt Schiff base complexes [34].

TABLE IX. Oxidation and Reduction Potentials of the $\mathrm{LCo(DH)_2N_3}$ and $\mathrm{LCo(DH)_2}$triazolate Complexes[a]

L	Co(III) ⇌ Co(IV)		Co(III) ⇌ Co(II)	
	$\mathrm{LCo(DH)_2N_3}$	$\mathrm{LCo(DH)_2}$triazolate	$\mathrm{LcO(DH)_2N_3}$	$\mathrm{LCo(DH)_2}$triazolate
$\mathrm{Me_2PPh}$	0.72(71)		−1.36(60)	
$\mathrm{(C_2H_5O)_3P}$	0.71(70)		−1.54[b]	
$\mathrm{1\text{-}CH_3Im}$	0.70(61)		−1.63[b]	
DBP	0.75(68)		−1.23(68)	
$\mathrm{MePPh_2}$	0.74(61)	0.77(67)	−1.30(62)	−1.39[b]
$\mathrm{P(n\text{-}Bu)_3}$	0.70(66)	0.76(87)	−1.36(65)	−1.36(55)
$\mathrm{(PhCH_2)_3P}$	0.73(84)		−1.31(104)	
$\mathrm{(C_6H_5O)_3P}$	0.71(88)		−1.55[b]	
Piperidine	0.69(60)		−1.54[b]	
Pyridine	0.74(71)	0.77(80)	−1.55[b]	−1.93[b]
$\mathrm{(C_6H_5)_3As}$	0.72(86)	0.78(72)	−1.40(92)	−0.94[b], −1.47[b], −1.77[b]
$(p\text{-}\mathrm{ClC_6H_4})_3\mathrm{P}$	0.74[c]		−1.18(72)	
$\mathrm{PPh_3}$	0.69[c]	0.56(65), 0.77(70), 0.996[b]	−1.24(84)	−0.48(148), −1.23(62), −1.82[b]
$(p\text{-}\mathrm{CH_3C_6H_4})_3\mathrm{P}$	0.73(88)	0.61[c, d]	−1.26(78)	−1.03[b], −1.25(102)[e]
$(p\text{-}\mathrm{CH_3OC_6H_4})_3\mathrm{P}$	0.70(77)		−1.27(77)	
$\mathrm{(C_6H_{11})_3P}$	0.76	0.96[c]	−1.35(98)	−1.73[b, d]

[a] In $\mathrm{CH_3CN}$ containing 0.1 M TEAP at 25 °C, $\nu = 200$ mV s^{-1}; data given as $E_{1/2}$ (V) *vs.* Fc$^+$/Fc; ($E_{\mathrm{pa}} - E_{\mathrm{pc}}$ (mV)). [b] E_{pc} only, fast followup chemical reaction. [c] E_{pa} only, fast followup chemical reaction. [d] Broad. [e] A third wave very near the limit was observed.

---

*This could mean that under the time domain of the electrochemical experiment the back reaction is not significant.

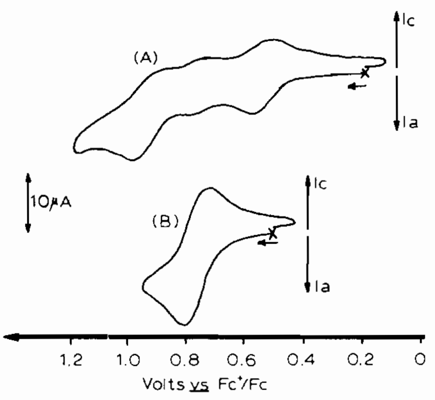

Fig. 5. Cyclic voltammograms for the oxidation of 1 × 10^{-3} M solutions of (A) $(C_6H_5)_3PCo(DH)_2$triazolate and (B) $MePPh_2Co(DH)_2$triazolate in CH_3CN (0.1 M TEAP; scan rate 500 mV s^{-1}) at 25 °C.

It may be seen from the data in Table IX that the ligand L in $LCo(DH)_2N_3$ has only a small influence on the oxidation potentials; however, it has a relatively much larger influence on the reduction potentials. In each case where the comparison may be made, it is more difficult to reduce the $LCo(DH)_2$triazolate complex than the $LCo(DH)_2N_3$ complex. This, in concert with the fact that the azide ligand is a very good bridging ligand for inner sphere electron transfer reactions [35] lends support to the mechanism proposed for the autocatalysis. Cyclic voltammetry provides additional support for the autocatalysis mechanism. Figure 5 illustrates different wave forms,

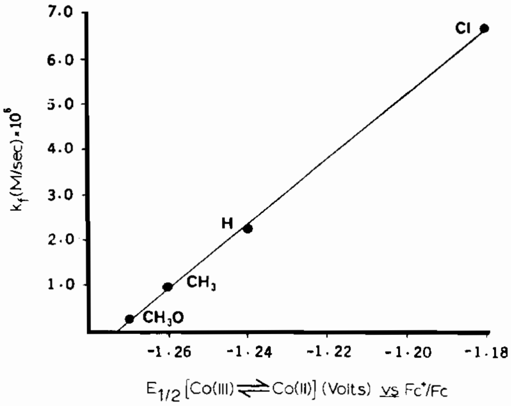

Fig. 6. Correlation between $E_{1/2}$ [Co(III)) ⇌ Co(II)] vs. Fc^+/Fc in acetonitrile containing 0.1 M TEAP at 25 °C for the $(p\text{-}XC_6H_4)_3PCo(DH)_2N_3$, X = CH_3O, CH_3, H, Cl complexes and k_f for the reaction of $(p\text{-}XC_6H_4)_3PCo(DH)_2N_3$ with $CH_3CO_2C{\equiv}CCO_2CH_3$ in $CHCl_3$ at 27 °C. k_f = 7.17 × 10^{-5} ($E_{1/2}$) + 9.13 × 10^{-5} (r^2 = 0.999).

corresponding to Co(III) ⇌ Co(IV) processes, for triazolate complexes which dissociate the ligand L [e.g. L = $(C_6H_5)_3P$) compared to those that do not (e.g. L = $MePPh_2$). For the $(C_6H_5)_3P$ complex, one can see distinct waves corresponding to three different species, one of which is probably $CH_3CNCo(DH)_2$triazolate (in such cases the redox potentials are only approximate). The $MePPh_2$ complex shows only one oxidation wave due to the single species $MePPh_2Co(DH)_2$triazolate. As may be seen from Fig. 5, the anodic currents in both cases are ap-

TABLE X. Spectroscopic Properties of $LCo(DH)_2N_3$ Complexes

L	θ[a]	$\nu(N_3)$(asym) in KBr (cm^{-1})	$\nu(N_3)$(asym) in $CHCl_3$ (cm^{-1})	$\nu(N_3)$(sym) in KBr (cm^{-1})	δ'H oxime[b] in $CDCl_3$ (ppm)	$\delta^{31}P$ ligand (ppm)	$\delta^{31}P$[c] complex (ppm)	$\Delta\delta^{31}P$[d]
Me_2PPh	127	2017	2022	1289	2.08	−47.0	28.5	75.5
$(C_2H_5O)_3P$	109	2019	2022	1294	2.35	137	97.5	−39.5
$1\text{-}CH_3Im$[e]		2030	2026	1291	2.37			
DBP[e]		2012	2020	1281	1.87	−10.7	30.7	41.4
$MePPh_2$	136	2021	2021	1284	1.98	−28.0	16.3	44.3
$P(n\text{-}Bu)_3$	132	2014	2021	1287	2.33	−33.3	24.2	57.5
$(PhCH_2)_3P$	136	2009	2019	1288	2.17	−12.9	19.5	32.4
$(C_5H_5O)_3P$	121	2012	2022	1283	2.10	125	90.8	−34.2
Piperidine		2020	2022	1294	2.47			
Pyridine		2019	2019	1281	2.33			
$(C_6H_5)_3As$	142	2006	2014	1283	2.08			
$(p\text{-}ClC_6H_4)_3P$	145	2009	2014	1283	2.05	−8.4	23.4	31.8
PPh_3	145	2007	2016	1285	2.00	−6.0	22.9	28.9
$(p\text{-}CH_3C_6H_4)_3P$	145	2012	2017	1287	2.02	−8.0	22.7	30.7
$(p\text{-}CH_3OC_6H_4)_3P$	145	2015	2017	1285	2.02	−10.4	21.7	32.1
$(C_6H_{11})_3P$	179	2005	2017	1290	2.37	−10.7	1.6	12.3

[a] Tolman's Cone Angle; see ref. 37. [b] J(PH) ~ 1 Hz for all R_3P containing complexes. [c] Because of the breadth of the reasonance δ ± 1 ppm. [d] $\Delta\delta^{31}P = \delta^{31}P(\text{complex}) - \delta^{31}P(\text{ligand})$; a negative coordination chemical shift is normal for phosphites; see ref. 38. [e] DBP, 1-phenyldibenzophosphole; $1\text{-}CH_3Im$, 1-methylimidazole.

proximately the same, indicating that several monoelectronic processes for a single $(C_6H_5)_3PCo(DH)_2$-triazolate species are not plausible.

If the rate determining step in the autocatalysis mechanism is inner sphere electron exchange involving reduction of $LCo^{III}(DH)_2N_3$ to $[LCo^{II}(DH)_2N_3]^-$ then one might expect that the easier it is to reduce the $LCo(DH)_2N_3$ species the faster will be the reaction [35] (greater k_f value). Indeed, there is an excellent linear correlation ($r^2 = 0.999$) between the k_f values and the $E_{1/2}$ values (Fig. 6) of the Co(III) $\rightleftharpoons$ Co(II) processes for the triarylphosphine azido complexes. Cyclic voltammetry experiments have also been performed on $(C_6H_5)_3PCo(DH)_2N_3$ and $(p\text{-}ClC_6H_4)_3PCo(DH)_2N_3$ in dichloromethane using 0.1 M tetrabutylammonium perchlorate as the supporting electrolyte. The order of both the oxidation and reduction potentials is the same in this solvent as in acetonitrile. Also, the rate of the chemical step following the heterogeneous charge transfer (dissociation of the ligand from the Co(IV) oxidized species) is lower in dichloromethane than in acetonitrile. Thus, the reverse reduction waves are seen in dichloromethane.

5. Relation of Spectroscopic Data to Reaction Rates

Spectrosocpic data and Tolman's Cone Angles (a measure of the steric size of the ligands L) for the complexes $LCo(DH)_2N_3$ are listed in Table X. Tolman's Cone Angle, the phosphorus coordination chemical shift and the value of $\nu(N_3)$(asym) may be used as guides for separating these compleces into the two categories of reaction. All complexes with cone angles for L less than 142°, phosphorus coordination chemical shifts greater than 32.1 ppm and $\nu(N_3)$(asym) in the vicinity of 2022 cm^{-1} react by an overall second order rate law of the form: rate = $k[LCo(DH)_2N_3][DAD]$. In contrast, those complexes with Tolman's Cone Angles greater than 142°, $\Delta\delta^{31}P$ less than 32.1 ppm, and $\nu(N_3)$(asym) in the vicinity of 2015 cm^{-1} react by an autocatalytic process. Thus, the larger the ligand, the weaker the cobalt ligand bond strength and the easier the dissociation of the ligand, the greater is the probability of the autocatalytic process if the dissociated ligand is a good enough nucleophile to react with DAD to form the cabenoid species.

Acknowledgements

Acknowledgement is made to the donors of the Petroleum Research Fund, administered by the American Chemical Society, to the UNR Research Advisory Board, to C.N.R. (Rome), Italy, the University of Trieste and to the Deutschen Forschungs Gemeinschaft and Fonds der Chemischen Industrie for financial support. We thank Professor H. E. LeMay, Jr. for helpful suggestions on the manuscript.

References

1 R. Huisgen, in A. Padwa (ed.), '1,3-Dipolar Cycloaddition Chemistry', Vol. 1, Wiley–Interscience, New York, 1984, Chap. 1; R. Huisgen, *J. Org. Chem., 41*, 403 (1976); R. Huisgen, *Angew. Chem., Int. Ed. Engl., 2*, 633 (1963).

2 T. Kemmerich, J. H. Nelson, N. E. Takach, H. Boehme, B. Jablonski and W. Beck, *Inorg. Chem., 21*, 1226 (1982).

3 N. E. Takach, E. M. Holt, N. W. Alcock, R. A. Henry, and J. H. Nelson, *J. Am. Chem. Soc., 102*, 2968 (1980).

4 N. E. Takach and J. H. Nelson, *Inorg. Chem., 20*, 1258 (1981).

5 (a) W. Beck, W. P. Fehlhammer, H. Bock and M. Bauder, *Chem. Ber., 102*, 3637 (1969); P. Kreutzer, Ch. Weis, H. Bohme, T. Kemmerich, W. Beck, C. Spencer and R. Mason, *Z. Naturforsch., 276*, 745 (1972); (b) P. H. Kreutzer, J. Cj. Weis, H. Bock, J. Erbe and W. Beck, *Chem. Ber., 116*, 2691 (1983); J. Erbe and W. Beck, *Chem. Ber., 116*, 3867 (1983).

6 G. I. Koldobskii, V. A. Ostrovskii and V. S. Popavskii, *Chem. Heterocycl. Comp. U.S.S.R. (Engl. Trans.), 18*, 965 (1982); *Khim. Geterotsikl. Soedin., 17*, 1299 (1981).

7 F. R. Benson, *Chem. Rev., 41*, 1 (1977).

8 K. Schofield, M. R. Grimmett and B. R. T. Keene, 'Heterocyclic Nitrogen Compounds; The Azoles', Cambridge University Press, New York, 1976.

9 R. J. Spear, *Aust. J. Chem., 37*, 2453 (1984), and refs. therein.

10 W. Beck, T. Kemmerich and H. Bohme, *Z. Naturforsch., Teil B, 34*, 200 (1979).

11 R. O. Lindsay and C. F. H. Allen, 'Organic Synthesis, Coll.', Vol. III, Wiley, New York, 1955, p. 710.

12 G. Gritzner and J. Kuta, 'Recommendations on Reporting Electrode Potentials in Nonaqueous Solvents', IUPAC, p. 1528.

13 R. R. Gagné, C. A. Koval and G. C. Lisensky, *Inorg. Chem., 19*, 2584 (1980).

14 P. N. Howells and J. H. Nelson, *J. Chem. Educ.*, 55, 311 (1978).

15 J. H. Nelson, N. E. Takach, N. Bresciani-Pahor, L. Randaccio and E. Zangrando, *Acta Crystallogr., Sect. C, 40*, 742 (1984).

16 R. Huisgen, G. Sziemies and L. Mobius, *Chem. Ber., 100*, 2492 (1967).

17 T. G. Appleton, H. C. Clark and L. E. Manzer, *Coord. Chem. Rev., 10*, 335 (1973).

18 J. K. Burdett and T. A. Albright, *Inorg. Chem., 18*, 2112 (1979).

19 M. M. Gofman and V. I. Nefodov, *Inorg. Chim. Acta, 28*, 1 (1978).

20 R. Ketari and A. Foucaud, *Tetrahedron Lett., 29*, 2563 (1978).

21 A. W. Johnson and J. C. Tebby, *J. Chem. Soc.*, 2126 (1961).

22 J. B. Hendrickson, R. Rees and J. F. Templeton, *J. Am. Chem. Soc., 86*, 107 (1964).

23 K. A. Rubinson, J. Caja, R. W. Hurst, E. Itabashi, T. M. Kenyhercz, W. R. Heineman and H. B. Mark Jr., *J. Chem. Soc., Chem. Commun.*, 47 (1980); T. M. Kenyhercz, T. P. Deangelis, B. J. Norris, W. R. Heineman and H. B. Mark Jr., *J. Am. Chem. Soc., 98*, 2469 (1976).

24 L. G. Marzilli, J. G. Salerno and L. A. Epps, *Inorg. Chem., 11*, 2050 (1972).

25 G. N. Schrauzer, *Inorg. Synth., 11*, 64 (1968).

26 L. G. Sillen and A. E. Martell, 'Stability Constants of Metal-ion Complexes', *Special Publication No. 25*, The Chemical Society, London, 1971; R. H. Abeles and D. Dolphin, *Acc. Chem. Res., 1*, 97 (1968).

27 A. Bigotto, G. Costa, G. Mestroni, G. Pellizer, A. Puxeddu, E. Reisenhofer, L. Stefani and G. Tauzher, *Inorg. Chim. Acta Rev.*, 41 (1970).

28 B. T. Hsieh, J. H. Nelson, E. B. Milosavljevic', W. Beck and T. Kemmerich, *Inorg. Chim. Acta, 133*, 267 (1987).

29 P. K. Kadaba, *Synthesis*, 71 (1973).

30 G. Costa, A. Puxeddu and G. Tauzher, *Inorg. Nucl. Chem. Lett., 4*, 319 (1968).

31 G. Costa, G. Mestroni, A. Puxeddu and E. Reisenhofer, *J. Chem. Soc. A*, 2870 (1970).

32 C. W. Smith, G. W. Vanloon and M. C. Baird, *J. Coord. Chem., 6*, 89 (1976).

33 R. S. Nicholson and I. Shain, *Anal. Chem., 36*, 706 (1964).

34 E. Reisenhofer and G. Costa, *Inorg. Chim. Acta, 49*, 121 (1981).

35 B. E. Douglas, D. H. McDaniel and J. J. Alexander, 'Concepts and Models of Inorganic Chemistry', 2nd edn., Wiley, New York, 1983, pp. 378–391.

36 H. H. Jaffe, *Chem. Rev., 53*, 191 (1953).

37 C. A. Tolman, *Chem. Rev., 77*, 313 (1977); W. C. Trogler and L. G. Marzilli, *Inorg. Chem., 14*, 1942 (1975).

38 J. G. Verkade, *Coord. Chem. Rev., 9*, 1 (1972/1973); J. Kargol, R. W. Crecely, J. L. Burmeister, P. J. Toscano and L. G. Marzilli, *Inorg. Chim. Acta, 40*, 79 (1980).